Hypersphere Fitting from Noisy Data Using an EM Algorithm

Julien Lesouple, Barbara Pilastre, Yoann Altmann, *Member, IEEE*, and Jean-Yves Tourneret, *Fellow, IEEE*

***Abstract*—This letter studies a new expectation maximization (EM) algorithm to solve the problem of circle, sphere and more generally hypersphere fitting. This algorithm relies on the introduction of random latent vectors having a priori independent von Mises-Fisher distributions defined on the hypersphere. This statistical model leads to a complete data likelihood whose expected value, conditioned on the observed data, has a Von Mises-Fisher distribution. As a result, the inference problem can be solved with a simple EM algorithm. The performance of the resulting hypersphere fitting algorithm is evaluated for circle and sphere fitting.**

***Index Terms*—Hypersphere Fitting, Maximum Likelihood Estimation, Expectation-Maximization Algorithm, von Mises-Fisher distribution.**

I. Introduction

Fitting a circle, a sphere or more generally an hypersphere to a noisy point cloud is a recurrent problem in many applications including object tracking [1]–[3], robotics [4]–[6] or image processing and pattern recognition [7]–[9]. Popular methods available in the literature are based on least squares [10]–[14] or maximum likelihood (ML) estimation [15], [16]. In the 2D case (circle fitting), the introduction of latent variables corresponding to the true location of the measurements on the circle allows the ML estimator of the center and radius of the circle to be approximated using a simple iterative algorithm [15]. In this paper, we extend this strategy to hypersphere fitting and introduce latent vectors defined as affine transformations of random vectors distributed according to a von Mises-Fisher distribution. These latent vectors allow the hypersphere fitting problem to be solved using a new expectation-maximization (EM) algorithm, which is the main contribution of this letter.

This letter is organized as follows. Section II introduces the ML formulation of the hypersphere fitting problem and the corresponding new EM algorithm. Section III evaluates the performance of this EM algorithm for circle and sphere fitting via a comparison with state-of-the-art methods on simulated data. Conclusion and future works are reported in Section IV.

J. Lesouple and B. Pilastre are with TéSA, 7 Boulevard de la Gare, 31500 Toulouse, France (e-mail: julien.lesouple@tesa.prd.fr).

Y. Altmann is with the School of Engineering, Heriot-Watt University, EH14 4AS Edinburgh, U.K. This work is partly supported by the Royal Academy of Engineering under the Research Fellowship scheme RF201617/16/31.

J.-Y. Tourneret is with the University of Toulouse, INP-ENSEEIHT/IRIT/TéSA, 2 Rue Charles Camichel, 31071 Toulouse France.

II. A New EM Algorithm for Hypersphere Fitting

A. Problem Formulation

Consider n noisy measurements $\boldsymbol{z}_i \in \mathbb{R}^d, i = 1, ..., n$ located around a hypersphere with radius r and center $\boldsymbol{c} \in \mathbb{R}^d$. We assume that the noise realizations corrupting the observations are mutually independent and distributed according to the same isotropic multivariate Gaussian distribution. The hypersphere fitting problem can then be formulated as an ML estimation problem by introducing latent vectors $\boldsymbol{x}_i \in \mathbb{R}^d, i = 1, ..., n$ corresponding to the true (and unknown) locations of the n points on the sphere, corrupted by an additive white Gaussian noise $\boldsymbol{n}_i$, i.e.,

$$\boldsymbol{z}_i = \boldsymbol{x}_i + \boldsymbol{n}_i, \tag{1}$$

where $\boldsymbol{n}_i \sim \mathcal{N}(\boldsymbol{0}_d, \sigma^2 \boldsymbol{I}_d)$, $\boldsymbol{0}_d$ is the zero vector of $\mathbb{R}^d$, σ^2 is the unknown noise variance and $\boldsymbol{I}_d$ is the $d \times d$ identity matrix. Since the vectors $\boldsymbol{x}_i$ are assumed to lie on the hypersphere of center $\boldsymbol{c}$ and radius r, they can be represented as affine transformations of unit vectors $\boldsymbol{u}_i \in \mathbb{R}^d$ (i.e., located on the hypersphere $\mathcal{H}_d$ of $\mathbb{R}^d$ defined by $\|\boldsymbol{u}_i\|_2 = 1$) such that

$$\boldsymbol{x}_i = \boldsymbol{c} + r\boldsymbol{u}_i. \tag{2}$$

These vectors $\boldsymbol{u}_i$ are assigned a von Mises-Fisher prior distribution denoted as $\boldsymbol{u}_i \sim \text{vMF}_d(\boldsymbol{u}_i; \boldsymbol{\mu}, \kappa)$ with density

$$f_d(\boldsymbol{u}_i; \boldsymbol{\mu}, \kappa) = C_d(\kappa) \exp\left(\kappa \boldsymbol{\mu}^T \boldsymbol{u}_i\right) 1_{\mathcal{H}}(\boldsymbol{u}_i), \tag{3}$$

where $\boldsymbol{\mu} \in \mathbb{R}^d$ is the mean direction (with $\|\boldsymbol{\mu}\| = 1$), $\kappa \geq 0$ is the concentration parameter and $C_d(\kappa)$ is a normalization constant. Note that this distribution reduces to the uniform distribution on the hypersphere for $\kappa = 0$. The hypersphere fitting problem thus consists of estimating the radius r and center $\boldsymbol{c}$ of the hypersphere $\mathcal{H}_d$ (and possibly the noise variance σ^2) from the measurements $\boldsymbol{Z} = \{\boldsymbol{z}_1, ..., \boldsymbol{z}_n\}$, given that the latent vectors $\boldsymbol{u}_i, i = 1, ..., n$ are also unknown.

B. Likelihood and complete likelihood

The conditional distribution of $\boldsymbol{z}_i$ given $\boldsymbol{u}_i$ is a Gaussian distribution with mean vector $\boldsymbol{x}_i = \boldsymbol{c} + r\boldsymbol{u}_i$ and covariance matrix $\sigma^2 \boldsymbol{I}_d$, i.e.,

$$\boldsymbol{z}_i | \boldsymbol{u}_i, \boldsymbol{\theta} \sim \mathcal{N}(\boldsymbol{c} + r\boldsymbol{u}_i, \sigma^2 \boldsymbol{I}_d), \tag{4}$$

where $\boldsymbol{\theta} = (r, \boldsymbol{c}^T, \sigma^2)^T$ contains the unknown parameters of interest of the proposed statistical model. The (marginal) likelihood of this model, which does not involve the latent vectors $\boldsymbol{u}_i$, is

$$\mathcal{L}(\boldsymbol{\theta}; \boldsymbol{Z}) = \prod_{i=1}^{n} p(\boldsymbol{z}_i | \boldsymbol{\theta}) = \prod_{i=1}^{n} \int_{\mathcal{H}_d} p(\boldsymbol{z}_i, \boldsymbol{u}_i | \boldsymbol{\theta}) d\boldsymbol{u}_i. \tag{5}$$

Straightforward computations allow $p(\boldsymbol{z}_i, \boldsymbol{u}_i|\boldsymbol{\theta})$ to be computed as follows

$$\begin{aligned} p(\boldsymbol{z}_i, \boldsymbol{u}_i|\boldsymbol{\theta}) &= p(\boldsymbol{z}_i|\boldsymbol{u}_i, \boldsymbol{\theta})p(\boldsymbol{u}_i) \\ &\propto (2\pi\sigma^2)^{-\frac{d}{2}} \exp\left(-\frac{1}{2\sigma^2}\left[\|\boldsymbol{z_i} - \boldsymbol{c}\|_2^2 + r^2\right]\right) \\ &\times \exp\left(\frac{r(\boldsymbol{z_i} - \boldsymbol{c})^T\boldsymbol{u}_i + \sigma^2\kappa\boldsymbol{\mu}^T\boldsymbol{u}_i}{\sigma^2}\right), \end{aligned} \tag{6}$$

where $\propto$ means "proportional to". This density can be integrated with respect to $\boldsymbol{u}_i$, using $\int_{\mathcal{H}_d} f_d(\boldsymbol{u}_i; \boldsymbol{\mu}_i, \kappa_i)d\boldsymbol{u}_i = 1$, where $f_d(\boldsymbol{u}_i; \boldsymbol{\mu}_i, \kappa_i)$ is the density of the Von Mises-Fisher distribution $\text{vMF}_d(\boldsymbol{u}_i; \boldsymbol{\mu}_i, \kappa_i)$ defined in (3) whose parameters are defined as

$$\kappa_i = \frac{\|\boldsymbol{\delta}_i\|_2}{\sigma^2}, \ \boldsymbol{\mu}_i = \frac{\boldsymbol{\delta}_i}{\|\boldsymbol{\delta}_i\|_2} \tag{7}$$

with $\boldsymbol{\delta}_i = r(\boldsymbol{z_i} - \boldsymbol{c}) + \sigma^2\kappa\boldsymbol{\mu}$. This leads to the following likelihood

$$\begin{aligned} \mathcal{L}\left(\boldsymbol{\theta}; \boldsymbol{Z}\right) &= \prod_{i=1}^{n} \int_{\mathcal{H}_d} p(\boldsymbol{z}_i|\boldsymbol{u}_i, \boldsymbol{\theta})p(\boldsymbol{u}_i)d\boldsymbol{u}_i \\ &\propto \frac{1}{(\sigma^2)^{\frac{nd}{2}}} \exp\left(-\frac{\sum_{i=1}^n\left[\|\boldsymbol{z_i} - \boldsymbol{c}\|_2^2 + r^2\right]}{2\sigma^2}\right) \prod_{i=1}^{n} \frac{I_{d/2-1}(\kappa_i)}{\kappa_i^{d/2-1}}, \end{aligned} \tag{8}$$

where $I_\nu(.)$ denotes the modified Bessel function of first kind of parameter ν [17, Chap. 10.25]. The ML estimator of the unknown parameter vector $\boldsymbol{\theta}$ maximizing (8) cannot be expressed in closed-form and cannot be computed easily using a numerical optimization method. This letter derives a new EM algorithm to solve more efficiently this estimation problem, which instead relies on the so-called complete likelihood defined as

$$\mathcal{L}_c\left(\boldsymbol{\theta}; \boldsymbol{Z}, \boldsymbol{U}\right) = \prod_{i=1}^{n} p(\boldsymbol{z}_i, \boldsymbol{u}_i|\boldsymbol{\theta}), \text{ with } \boldsymbol{U} = \{\boldsymbol{u}_1, ..., \boldsymbol{u}_n\}. \tag{9}$$

C. Proposed EM Algorithm

The EM algorithm alternates between two steps referred to as expectation (E) and maximization (M) steps that are recalled below for iteration $(t+1)$ [18]

1- The E-step consists of computing $Q(\boldsymbol{\theta}|\boldsymbol{\theta}^{(t)})$, the expected value of the complete data log-likelihood given the observed data and the current parameter estimate $\boldsymbol{\theta}^{(t)}$, defined as

$$Q(\boldsymbol{\theta}|\boldsymbol{\theta}^{(t)}) = \mathbb{E}_{\boldsymbol{U}|\boldsymbol{Z},\boldsymbol{\theta}^{(t)}}\left[\log\mathcal{L}_c\left(\boldsymbol{\theta}; \boldsymbol{Z}, \boldsymbol{U}\right)\right]. \tag{10}$$

2- The M-step consists of estimating $\boldsymbol{\theta}^{(t+1)}$ by solving

$$\boldsymbol{\theta}^{(t+1)} = \arg\max_{\boldsymbol{\theta}} Q(\boldsymbol{\theta}|\boldsymbol{\theta}^{(t)}). \tag{11}$$

The complete data likelihood can be computed using (9) and (6). Straightforward computations lead to

$$\begin{aligned} \log\mathcal{L}_c\left(\boldsymbol{\theta}; \boldsymbol{Z}, \boldsymbol{U}\right) &= K - \frac{nd}{2}\log(\sigma^2) \\ &- \frac{1}{2\sigma^2}\sum_{i=1}^{n}\left[\|\boldsymbol{z}_i - \boldsymbol{c}\|_2^2 + r^2 - 2\boldsymbol{\delta}_i^T\boldsymbol{u}_i\right], \end{aligned} \tag{12}$$

where K is a constant (independent of $\boldsymbol{\theta}$ and $\boldsymbol{U}$). Using (12) leads to

$$\begin{aligned} Q(\boldsymbol{\theta}|\boldsymbol{\theta}^{(t)}) &= K - \frac{nd}{2}\log(\sigma^2) \\ &- \frac{1}{2\sigma^2}\sum_{i=1}^{n}\left\{\|\boldsymbol{z}_i - \boldsymbol{c}\|_2^2 + r^2 - 2\boldsymbol{\delta}_i^T\mathbb{E}_{\boldsymbol{U}|\boldsymbol{Z},\boldsymbol{\theta}^{(t)}}\left[\boldsymbol{u}_i\right]\right\}. \end{aligned} \tag{13}$$

The distribution of $\boldsymbol{U}|\boldsymbol{Z}, \boldsymbol{\theta}^{(t)}$ can then be determined using

$$p(\boldsymbol{U}|\boldsymbol{Z}, \boldsymbol{\theta}^{(t)}) \propto \prod_{i=1}^{n} p(\boldsymbol{z}_i|\boldsymbol{u}_i, \boldsymbol{\theta}^{(t)})p(\boldsymbol{u}_i). \tag{14}$$

The marginal distribution of $\boldsymbol{u}_i|\boldsymbol{Z}, \boldsymbol{\theta}^{(t)}$ is the von Mises-Fisher distribution $\text{vMF}_d(\boldsymbol{u}_i; \boldsymbol{\mu}_i, \kappa_i)$, whose expectation is given by [19, Chap. 9.3.2]

$$\mathbb{E}_{\boldsymbol{U}|\boldsymbol{Z},\boldsymbol{\theta}^{(t)}}\left(\boldsymbol{u}_i\right) = \frac{I_{d/2}\left[\kappa_i^{(t)}\right]}{I_{d/2-1}\left[\kappa_i^{(t)}\right]}\boldsymbol{\mu}_i^{(t)}, \tag{15}$$

where $\boldsymbol{\mu}_i^{(t)}$ and $\kappa_i^{(t)}$ are computed from (7) using the current values of $r, \boldsymbol{c}$ and σ^2. After substituting this expectation into (13), the maximization of the function $Q(\boldsymbol{\theta}|\boldsymbol{\theta}^{(t)})$ with respect to $\boldsymbol{\theta}$ leads to the following updates for r, $\boldsymbol{c}$ and σ

$$\begin{bmatrix} r^{(t+1)} \\ \boldsymbol{c}^{(t+1)} \end{bmatrix} = (\boldsymbol{H}^{(t)})^{-1}\boldsymbol{f}^{(t)}, \ \sigma^{(t+1)} = \sqrt{\frac{M^{(t+1)}}{nd}}, \tag{16}$$

where

$$\boldsymbol{\alpha}_i^{(t)} = \frac{I_{d/2}\left[\kappa_i^{(t)}\right]}{I_{d/2-1}\left[\kappa_i^{(t)}\right]}\boldsymbol{\mu}_i^{(t)}, \boldsymbol{f}^{(t)} = \begin{bmatrix} \sum_{i=1}^n(\boldsymbol{\alpha}_i^{(t)})^T\boldsymbol{z}_i \\ \sum_{i=1}^n \boldsymbol{z}_i \end{bmatrix}, \tag{17}$$

$$\boldsymbol{H}^{(t)} = \begin{bmatrix} n & \sum_{i=1}^n(\boldsymbol{\alpha}_i^{(t)})^T \\ \sum_{i=1}^n \boldsymbol{\alpha}_i^{(t)} & nI_d \end{bmatrix}, \tag{18}$$

$$M^{(t+1)} = \sum_{i=1}^{n}\|\boldsymbol{z}_i\|_2^2 - (\boldsymbol{f}^{(t)})^T\begin{bmatrix} r^{(t+1)} \\ \boldsymbol{c}^{(t+1)} \end{bmatrix}. \tag{19}$$

Note that the matrix $\boldsymbol{H}^{(t)}$ is invertible. Introducing $\boldsymbol{\alpha}^{(t)} = \sum_{i=1}^n \boldsymbol{\alpha}_i^{(t)}$, its inverse can be computed as follows [20]

$$(\boldsymbol{H}^{(t)})^{-1} = \frac{1}{n^2 - \boldsymbol{\alpha}^T\boldsymbol{\alpha}}\begin{bmatrix} n & -\boldsymbol{\alpha}^T \\ -\boldsymbol{\alpha} & \frac{n^2 - \boldsymbol{\alpha}^T\boldsymbol{\alpha}}{n}I_d + \frac{1}{n}\boldsymbol{\alpha}\boldsymbol{\alpha}^T \end{bmatrix}. \tag{20}$$

III. EXPERIMENTS

This section evaluates the performance of the proposed EM algorithm for circle and sphere fitting, which allows a comparison with the state-of-the-art. The different approaches are applied on a simulated point cloud of $n = 100$ latent vectors uniformly distributed on the circle or the sphere (i.e., with a von-Mises Fisher distribution with concentration parameter $\kappa = 0$). These latent vectors are then corrupted by a zero-mean Gaussian noise with covariance matrix $\sigma^2 I_d$. For each run, the coordinates of the true center and the radius are chosen uniformly in the intervals $[5, 10]$ and $[1, 10]$. The EM algorithm is iterative and requires to be initialized properly. In all the experiments, the center has been initialized by the mean of the noisy measurements denoted as $\boldsymbol{c}_0$, the initial radius has been fixed to its MLE given $\boldsymbol{c}_0$, i.e., $r_0 = \frac{1}{n}\sum_{i=1}^{n} \|\boldsymbol{z}_i - \boldsymbol{c}_0\|$, and the noise variance by its MLE given $(\boldsymbol{c}_0, r_0)$, i.e., $\sigma_0^2 = \frac{1}{nd}\sum_{i=1}^{n} \|\boldsymbol{z}_i - \boldsymbol{c}_0\|^2 - \frac{1}{d}r_0^2$. Note again that the MLE of $\boldsymbol{\theta} = (r, \boldsymbol{c}^T, \sigma^2)^T$ does not admit a closed-form expression for the proposed statistical model.

A. *Circle Fitting with a uniform prior*

The first experiments illustrate the convergence of the proposed EM algorithm for circle fitting from noisy measurements with a noise variance $\sigma^2 = 0.1$. Fig. 1 shows the global mean square error (MSE) of $\boldsymbol{\theta}$ (computed by averaging the results of 500 Monte Carlo run) with the corresponding error bars, for the first 20 iterations of the EM algorithm. The proposed method seems to converge close to the actual value of $\boldsymbol{\theta}$, even if the EM algorithm is known to only converge to a local maximum of the likelihood.

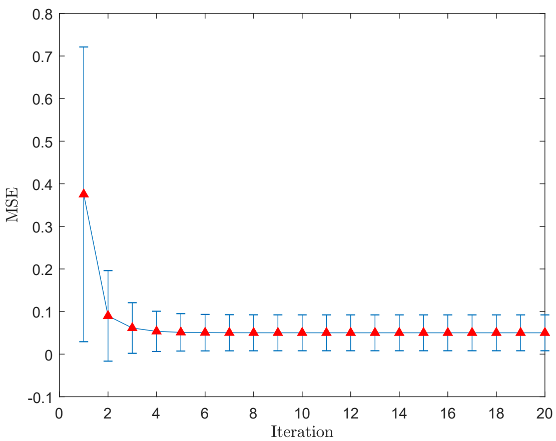

Fig. 1. MSE of $\widehat{\boldsymbol{\theta}} = (\hat{r}, \hat{\boldsymbol{c}}^T, \hat{\sigma})^T$ for the first 20 iterations of the proposed EM algorithm applied to circle fitting ($n = 100$ and $\sigma^2 = 0.1$).

The proposed EM algorithm is compared with three state-of-the-art methods: 1) the Exact-Landau (E-Landau) algorithm [11] (an extension of the iterative solution of [12]), 2) the modified least squares estimator [21] (referred to as "Kasa" hereafter) and 3) the iterative maximum likelihood (IML) estimator [15]. The two first methods compute closed-form solutions obtained using least squares methods as defined in [11] and [21]. The third approach solves the circle fitting problem using a simple iterative algorithm computing an approximate ML estimator. Fig. 2 shows the global mean square error (MSE) of $\widehat{\boldsymbol{\theta}} = (\hat{r}, \hat{\boldsymbol{c}}^T)^T$ versus the noise variance σ^2. All the methods perform very similarly for small values of σ^2. The advantage of the proposed EM algorithm can be observed for high noise levels ($\sigma^2 > 0.3$ here), where the MSE of the estimated vector $\widehat{\boldsymbol{\theta}}$ is smaller with the proposed method, showing more robustness to the presence of noise. More simulation results including MSE comparisons for the estimates of $\boldsymbol{c}$, r and σ^2 are available in [20].

B. *Sphere Fitting with a uniform prior*

This section evaluates the performance of the proposed EM algorithm for sphere fitting. The global mean square error

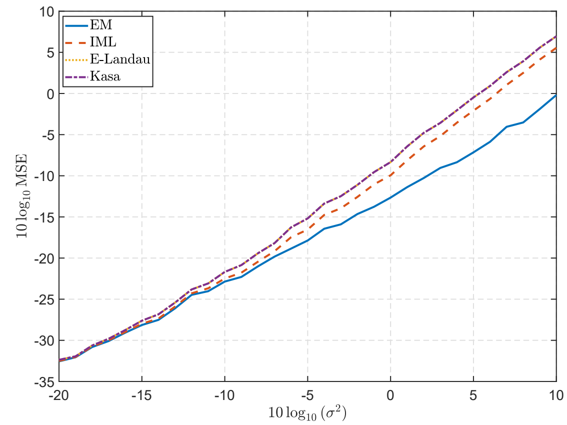

Fig. 2. MSE of $\widehat{\boldsymbol{\theta}} = (\hat{r}, \hat{\boldsymbol{c}}^T)^T$ for E-Landau, Kasa, IML and EM (proposed method) versus noise power σ^2 (500 Monte Carlo runs).

(MSE) of $\widehat{\boldsymbol{\theta}}$ and the corresponding error bars are displayed in Fig. 3 for the first twenty iterations of the EM algorithm, showing good convergence properties. Two state-of-the-art approaches are then considered for comparison purposes: 1) the fast geometric fit algorithm (FGFA) [22] and 2) the Iterative least squares approach [14], which are extensions of the E-Landau [11] and IML [15] algorithms for the 3D case. The results of Fig. 4 are similar to those obtained for circle fitting, i.e., the algorithms perform similarly for small noise variances and the proposed EM algorithm provide better results for more noisy scenarios.

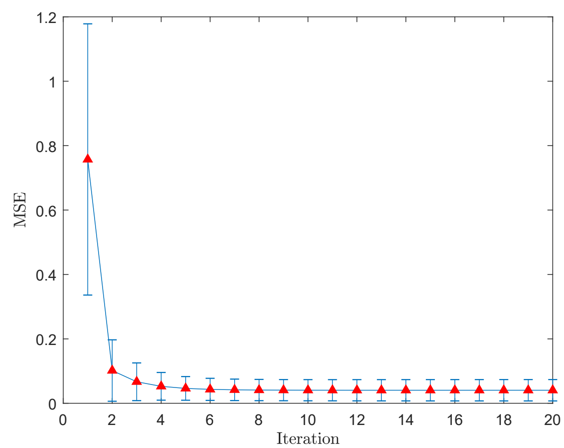

Fig. 3. MSE of $\widehat{\boldsymbol{\theta}} = (\hat{r}, \hat{\boldsymbol{c}}^T, \hat{\sigma})^T$ for the first 20 iterations of the proposed EM algorithm applied to sphere fitting ($n = 100$ and $\sigma^2 = 0.1$).

C. *Hypersphere fitting with a Von Mises-Fisher prior*

In some applications including LIDAR-based 3D imaging [23], [24], the spheres present in the scene are not sampled uniformy. More specifically, for long-range imaging applications where the field of view is particularly narrow, it is possible to define an average beam direction, which can be used as the mean direction $\boldsymbol{\mu}$ of the Von Mises-Fisher prior, as opposed to a uniform prior. This section considers 2D and 3D experiments corresponding to von Mises-Fisher priors with parameters $\boldsymbol{\mu} = [\cos(\pi/4), \sin(\pi/4)]^T$ (2D) and

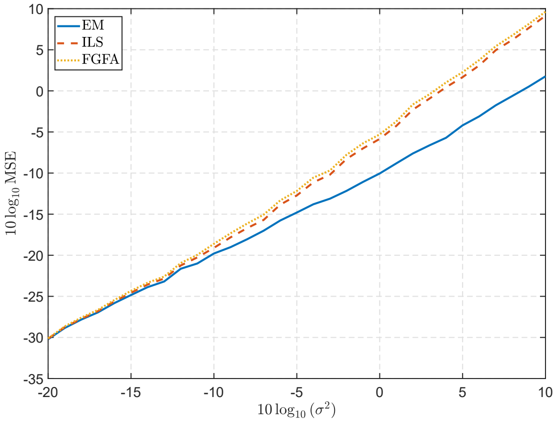

Fig. 4. MSE of $\widehat{\boldsymbol{\theta}} = (\hat{r}, \hat{\boldsymbol{c}}^T)^T$ for ILS, FGFA and EM (proposed method) versus noise power σ^2 (results averaged over 500 Monte Carlo runs).

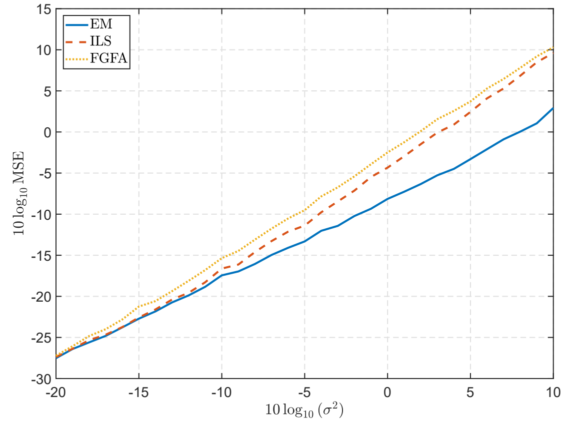

Fig. 6. MSEs of $\hat{\boldsymbol{\theta}} = (\hat{r}, \hat{\boldsymbol{c}}^T)^T$ for FGFA, ILS and EM (proposed method) versus noise power σ^2 (500 Monte Carlo runs) for a von Mises-Fisher prior ($\boldsymbol{\mu} = [\sin(\pi/4)\cos(\pi/3), \sin(\pi/4)\sin(\pi/3), \cos(\pi/4)]^T$ and $\kappa = 2$).

$\boldsymbol{\mu} = [\sin(\pi/4)\cos(\pi/3), \sin(\pi/4)\sin(\pi/3), \cos(\pi/4)]^T$ (3D), and $\kappa = 2$. The MSEs of $\hat{\boldsymbol{\theta}}$ obtained using the different estimation algorithms for these two scenarios are displayed in Figs. 5 and 6. As one can see, the proposed method provides competitive results compared to the state-of-the-art.

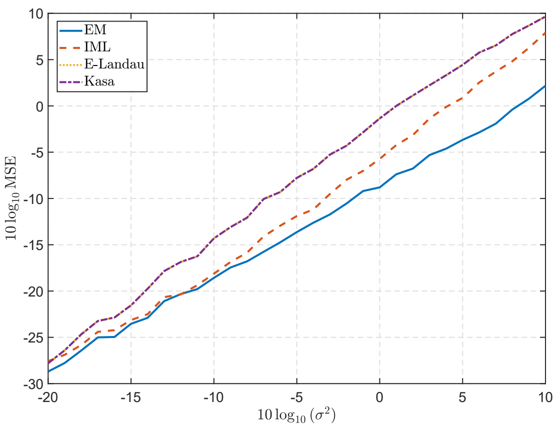

Fig. 5. MSEs of $\hat{\boldsymbol{\theta}} = (\hat{r}, \hat{\boldsymbol{c}}^T)^T$ for E-Landau, Kasa, IML and EM (proposed method) versus noise power σ^2 (500 Monte Carlo runs) for a von Mises-Fisher prior ($\boldsymbol{\mu} = [\cos(\pi/4), \sin(\pi/4)]^T$ and $\kappa = 2$).

D. Discussions

1) Computational complexity: This section first compares the execution times of the different hypersphere fitting algorithms, which are reported in Table I with the corresponding standard deviations computed using 500 Monte-Carlo runs. Note that the number of iterations has been fixed to 40 for the iterative algorithms (proposed EM, ILS and IML) and that the simulation scenario is the same as in Sections III A and B. Even if the execution times of the proposed EM algorithm are larger than those obtained with the other benchmarks, they remain reasonable for practical applications.

TABLE I
AVERAGED EXECUTION TIMES (IN MICROSECONDS) WITH THEIR STANDARD DEVIATIONS FOR THE VARIOUS METHODS.

2D	E-Landau	Kasa	ILS	EM
Time	46 ± 40	22 ± 40	950 ± 300	6400 ± 2000
3D		FGFA	IML	EM
Time		16 ± 20	930 ± 200	6200 ± 2000

2) Generalizations to hyper-ellipsoid fitting/colored noise: In order to extend the proposed EM algorithm to hyper-ellipsoid fitting, one can use the following parametrization of the ellipsoid

$$\boldsymbol{z}_i = \boldsymbol{c} + \boldsymbol{A}\boldsymbol{u}_i + \boldsymbol{n}_i,$$

where $\boldsymbol{c}$ is the ellipsoid center, $\boldsymbol{A}$ is a positive definite matrix and $\boldsymbol{u}_i$ is a latent vector located on the unit hypersphere. In this case, the hyper-ellipsoid fitting problem reduces to estimating the parameters $\sigma^2, \boldsymbol{c}$ and the matrix $\boldsymbol{A}$ from the observed vectors $\boldsymbol{z}_i$. The presence of the matrix $\boldsymbol{A}$ complicates the problem significantly since the marginal distribution of $\boldsymbol{u}_i|\boldsymbol{Z}, \boldsymbol{\theta}^{(t)}$ is no longer a von Mises-Fisher distribution. The same problem occurs in the case of a non-isotropic Gaussian noise whose covariance matrix is different from $\sigma^2 I_d$. Generalizing the EM algorithm to these situations is an interesting prospect, which would be useful for object tracking applications [2].

IV. CONCLUSION

This paper proposed a new EM algorithm for hypersphere fitting in any dimension based on maximum likelihood estimation. The algorithm was derived after introducing latent variables corresponding to the true locations of the measurements on the hypersphere and assuming that these variables have a von Mises-Fisher distribution. The proposed algorithm was evaluated for circle and sphere fitting allowing a comparison with state-of-the-art methods. The results obtained on simulated data are encouraging and show the competitiveness of the proposed approach. Future work includes the development of a robust version of the method to handle the presence of potential outliers and the generalization of the method to ellipsoid fitting or colored noise. Using the proposed algorithm for the calibration of LIDARs or developing a sequential version for object tracking are also interesting problems. Finally, estimating the hyperparameters of the von Mises-Fisher distribution jointly with the parameters of the hypersphere is a challenging issue, which would avoid the hyperparameters of the latent vectors prior to be adjusted.

REFERENCES

[1] D. Epstein and D. Feldman, “Sphere Fitting with Applications to Machine Tracking,” *Algorithms*, vol. 13, no. 8, p. 177, July 2020.

[2] M. Baum and U. D. Hanebeck, “Extended Object Tracking with Random Hypersurface Models,” *IEEE Trans. Aerosp. Electron. Syst.*, vol. 50, no. 1, pp. 149–159, Jan. 2014.

[3] N. Wahlström and E. Özkan, “Extended Target Tracking Using Gaussian Processes,” *IEEE Trans. Aerosp. Electron. Syst.*, vol. 50, no. 1, pp. 4165–4178, May 2015.

[4] F. Sandoval, “An Algorithm for Fitting 2-D Data on the Circle: Applications to Mobile Robotics,” *IEEE Signal Process. Lett.*, vol. 15, pp. 127–130, Jan. 2008.

[5] D. Epstein and D. Feldman, “Quadcopter Tracks Quadcopter via Real Time Shape Fitting,” *IEEE Robot. Autom. Lett.*, vol. 3, p. 544550, Jan. 2018.

[6] F. Bonin-Font, A. Ortiz, and G. Oliver, “Visual Navigation for Mobile Robots: A Survey,” *J. Intell. Robot. Syst.*, vol. 53, p. 263296, Nov. 2008.

[7] D. Lin and C. Yang, “Real-Time Eye Detection Using Face-Circle Fitting and Dark-Pixel Filtering,” in *Proc. IEEE Int. Conf. on Multimedia ans Expo (ICME’2004)*, Taipei, Taiwan, June 2004, pp. 1167–1170.

[8] A. Geiger, P. Lenz, and R. Urtasun, “Are We Ready for Autonomous Driving? The Kitti Vision Benchmark Suite,” in *Proc. IEEE Int. Conf. Conf. Comput. Vis. Pattern Recognit. (CVPR’2012)*, Providence, RI, USA, Jun. 2012, pp. 3354–3361.

[9] L. Pan, W. Chu, J. M. Saragih, F. De la Torre, and M. Xie, “Fast and Robust Circular Object Detection With Probabilistic Pairwise Voting,” *IEEE Sign. Process. Let.*, vol. 18, no. 11, pp. 639–642, Sept. 2011.

[10] D. Umbach and K. Jones, “A Few Methods for Fitting Circle to Data,” *IEEE Trans. Instrum. Meas.*, vol. 52, pp. 1881–1885, June 2003.

[11] Y. S. Thomas and A. Chan, “Simple Approach for the Estimation of Circular Arc Center and Its Radius,” *Computer Vision, Graphics, and Image Processing*, vol. 45, pp. 362–370, Mar. 1989.

[12] U. Landau, “Estimation of a Circular Arc Center and its Radius,” *Computer Vision, Graphics, and Image Processing*, vol. 38, pp. 317–326, June 1987.

[13] G. Golub, “Hyperspheres and Hyperplanes Fitted Seamlessly by Algebraic Constrained Total Least-Squares,” *Linear Algebra and its Applications*, vol. 331, no. 1-3, pp. 43–59, July 2001.

[14] D. Eberly, “Least Squares Fitting of Data,” Magic Software, Chapel Hill, NC, USA, Tech. Rep., Aug. 2000. [Online]. Available: http://www.geometrictools.com

[15] W. Li, J. Zhong, T. A. Gulliver, B. Rong, R. Hu, and Y. Qian, “Fitting Noisy Data to a Circle: A Simple Iterative Maximum Likelihood Approach,” in *Proc. IEEE Int. Conf. on Communications*, July 2011, pp. 1 – 5.

[16] E. E. Zelniker and I. V. L. Clarkson, “Maximum-Likelihood Estimation of Circle Parameters via Convolution,” *IEEE Trans. Image Process.*, vol. 15, no. 4, pp. 865–876, Apr. 2006.

[17] F. W. J. Olver, D. W. Lozier, R. F. Boisvert, and C. W. Clark, *NIST Handbook of Mathematical Functions*. Cambridge University Press, 2010.

[18] A. Dempster, N. Laird, and D. Rubin, “Maximum Likelihood from Incomplete Data via the EM Algorithm,” *J R Stat Soc Series B*, vol. 39, no. 1, pp. 1–38, 1977.

[19] K. V. Mardia and P. E. Jupp, *Directional Statistics*. John Wiley & Sons, Inc., 1999.

[20] J. Lesouple, B. Pilastre, Y. Altmann, and J.-Y. Tourneret, “Hypersphere Fitting from Noisy Data Using an EM Algorithm - Supplementary Material,” TéSA Laboratory, Toulouse, France, Tech. Rep., Aug. 2020. [Online]. Available: http://perso.tesa.prd.fr/jlesouple/documents/TRhypersphere2020.pdf

[21] I. Kasa, “A Circle Fitting Procedure and Its Error Analysis,” *IEEE Trans. Instrum. Meas.*, vol. IM-25, no. 1, pp. 8–14, Mar. 1976.

[22] Y. Sumith, “Fast Geometric Fit Algorithm for Sphere Using Exact Solution,” *CoRR*, 2015.

[23] T. Tóth, Z. Pusztai, and L. Hajder, “Automatic LiDAR-camera calibration of extrinsic parameters using a spherical target,” in *Proc. IEEE Int. Conf. on Robotics and Automation (ICRA’2020)*, Paris, France, MAy 31 - Aug. 31 2020.

[24] Y. Wang, H. Shi, Y. Zhang, and D. Zhang, “Automatic registration of laser point clouds using precisely located sphere targets,” *J. Applied Remote Sens.*, vol. 8, no. 1, July 2014.